

Photon-induced degradation of InGaN-based LED in open-circuit conditions investigated by steady-state phot capacitance and photoluminescence

Cite as: J. Appl. Phys. **131**, 043102 (2022); doi: [10.1063/5.0079022](https://doi.org/10.1063/5.0079022)

Submitted: 17 November 2021 · Accepted: 7 January 2022 ·

Published Online: 25 January 2022



Alessandro Caria,^{a)} Carlo De Santi, Matteo Buffolo, Gaudenzio Meneghesso, Enrico Zanoni, and Matteo Meneghini

AFFILIATIONS

Department of Information Engineering, University of Padova, Via G. Gradenigo 6/B, 35131 Padova, Italy

^{a)}Author to whom correspondence should be addressed: alessandro.caria@dei.unipd.it

ABSTRACT

Degradation of InGaN–GaN LEDs has been the subject of intense investigations in the past few years. While current- and temperature-induced degradation processes have been described, the impact of photon-induced degradation has not been investigated in detail in the literature. This paper aims at improving the understanding of the mechanisms responsible for the degradation of the InGaN subject to high photon densities by stressing the devices under a high-intensity laser beam in open-circuit conditions (i.e., in the absence of external current). We analyzed the degradation by means of electrical, optical, and deep-level characterization techniques. First, we demonstrate the existence of optically induced degradation processes in GaN LEDs: from photoluminescence measurements, we observed a decrease in the luminescence after stress, more prominent in the region irradiated during stress. Second, we ascribe this effect to a decrease in internal quantum efficiency due to the generation of non-radiative defects within the active region. Third, by steady-state phot capacitance measurements, we reveal the presence of a shallow level with an energy of $E_C-2.2$ eV, which can be ascribed to gallium vacancies and its complexes with oxygen and nitrogen and can be related to the increase in yellow luminescence.

Published under an exclusive license by AIP Publishing. <https://doi.org/10.1063/5.0079022>

INTRODUCTION

Gallium nitride-based LEDs created a revolution in the optoelectronics field, enabling the fabrication of blue-emitting diodes, whose emission is easily converted into white light by means of phosphors. A number of studies investigated the reliability of these devices, focusing on the root cause of degradation and analyzing different failure mechanisms,^{1–3} such as the degradation of the ohmic contacts,⁴ the creation of defects in the material,^{5,6} and the failure of devices submitted to extremely high current/temperature levels.^{7,8} The experiments were carried out also as a function of the stress conditions and in view of the final application.^{9–11}

While the effect of high current densities and temperatures on LED degradation has been widely investigated, the impact of optically induced degradation has not been explored in the literature. The question is: can defect generation be promoted by the presence

of highly energetic photons? This question is of particular importance for short-wavelength LEDs (InGaN-based or AlGaIn-based) for which photon energies may be higher than 2.5–3 eV, i.e., comparable to the energy necessary for the creation of defects, which, under specific conditions, has been reported to be as low as 1.56 eV.¹²

Optically induced defect generation is of great concern: in fact, currently developed LEDs can reach extremely high optical power densities, which can exceed 50–100 W/cm²,¹³ corresponding to photon fluxes $>10^{20}$ photons/(cm² s). Exploring the impact of such high optical density levels on LED reliability is thus of fundamental importance for the development of long-lifetime LEDs.

The goal of this article is to make a step forward in this field by presenting the first demonstration of optically induced degradation in InGaN-based light emitting diodes.

To avoid current-induced degradation processes, we stressed the devices at high optical field in open-circuit conditions. In this way, current flow is minimized, and degradation is mainly promoted by optical excitation. Optical excitation was obtained through an external laser diode: photon energy was selected with the aim of generating carriers only in the quantum wells, thus maximizing (in the laser spot) the recombination rate. The laser spot was kept smaller than the LED area to maximize excitation intensity and to be able to detect a contrast between stressed and unstressed areas.

EXPERIMENTAL DETAILS

The devices under test are commercial $330 \times 330 \mu\text{m}^2$ GaN LED chips on a sapphire substrate emitting at 430 nm. No information on the epitaxial structure is available by the manufacturer, but this does not limit the generality of the analysis, showing that the observed processes are detected also in state-of-the-art technologies. The samples are optically stressed by means of a 405 nm laser diode (nominal optical power > 2 W), enclosed in a TEC-cooled laser fixture. The TEC cooler and the LD are driven by a controller. A part of the collimated laser beam is deflected by a beam sampler to a photodiode to provide an optical feedback of the laser beam power, ensuring its stability during long-term stresses. The laser beam is then reflected by a mirror and focused by a lens on the sample. The optical power of the beam is measured by a calibrated integrating sphere. The setup is schematized in Fig. 1. The focused beam power profile is measured by a CCD camera, obtaining a nearly circular shape with a diameter around $90 \mu\text{m}$, visible in Fig. 6(e).

During stress, the device was kept in open-circuit conditions. A switch matrix was used to disconnect the sample during the stress and to connect it to a semiconductor parameter analyzer and to a LCR meter for electrical and capacitance characterization, respectively.

The device was stressed for 35 000 min (around 583 h) at a constant optical power of 0.766 W, corresponding to an intensity of around $12\,000 \text{ W/cm}^2$, assuming—in approximation—that all the optical power is uniformly distributed in the laser spot. After each step of the stress, the device was characterized by means of I–V, L–I, C–V, and steady-state photocapacitance (SSPC) measurements.

A 405 nm LD, similar to the one used for the stress, was used for photoluminescence measurements. The light emitted by the

device was filtered to obtain a monochromatic emission and acquired by an EM-CCD camera.

DISCUSSION

From the I–V characterization [Fig. 2(a)], it is possible to see an increase in reverse leakage and low forward bias current [Fig. 2(b)]. This increase can be attributed to an increase in trap-assisted tunneling mechanisms. In fact, previous reports indicated that the sub-turn-on voltage region of the I–V characteristics is particularly sensitive to the presence of midgap states, which can result in enhanced trap-assisted tunneling components.^{14–16} From the analysis of the I–V curves, we further notice that the series resistance has negligible changes during the stress (i.e., there is no variation in the I–V curve slope at high current levels), suggesting that the electrical contacts of the devices are not affected by the adopted stress conditions.⁴

Optical power during the stress, shown in Fig. 3(a), has relevant variations only at low characterization current. In this operating regime, there is an initial increase in optical power [during the first 100 min of stress, see Fig. 3(b)], followed by a significant decrease in the luminescence signal. At higher measuring currents, no relevant degradation was identified. Similar information was obtained by the normalized pseudo-efficiency data, defined as the ratio between optical power and driving current [Fig. 3(c)]. The stronger degradation detected at low current is ascribed to the generation of non-radiative recombination centers (NRCs), whose effect is to decrease the non-radiative lifetime of the devices. In the low current regime (where Auger recombination is—in a first order approximation—neglected), the recombination rate is dependent on the Shockley–Read–Hall (SRH) and bimolecular recombination rates according to

$$\frac{1}{\tau} = \frac{1}{\tau_{\text{SRH}}} + \frac{1}{\tau_r} \sim N_T v_{th} \sigma + B n^2, \quad (1)$$

where τ_{SRH} is the SRH recombination rate, τ_r is the radiative recombination rate, N_T is the density of defects responsible for non-radiative recombination, v_{th} is the carrier thermal velocity, σ is the corresponding capture cross section, B is the radiative recombination rate, and n is the density of carriers in the active region. At low carrier densities, the term $B n^2$ is small, and a variation in trap density N_T may significantly impact on carrier lifetime. On the other hand, at high current levels, the recombination rate is

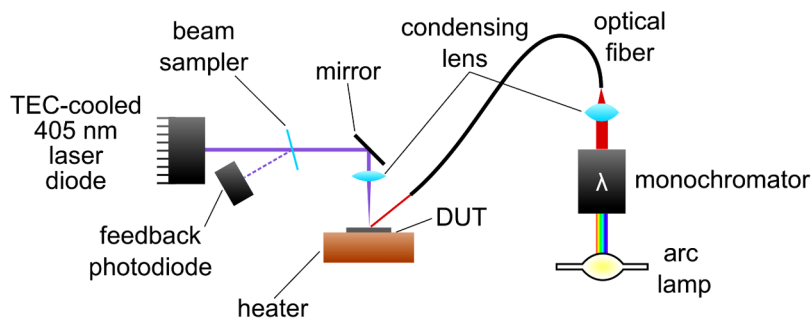


FIG. 1. Drawing of the experimental setup used for stress and characterization. A switch matrix, an LCR meter, and a semiconductor parameter analyzer are not shown.

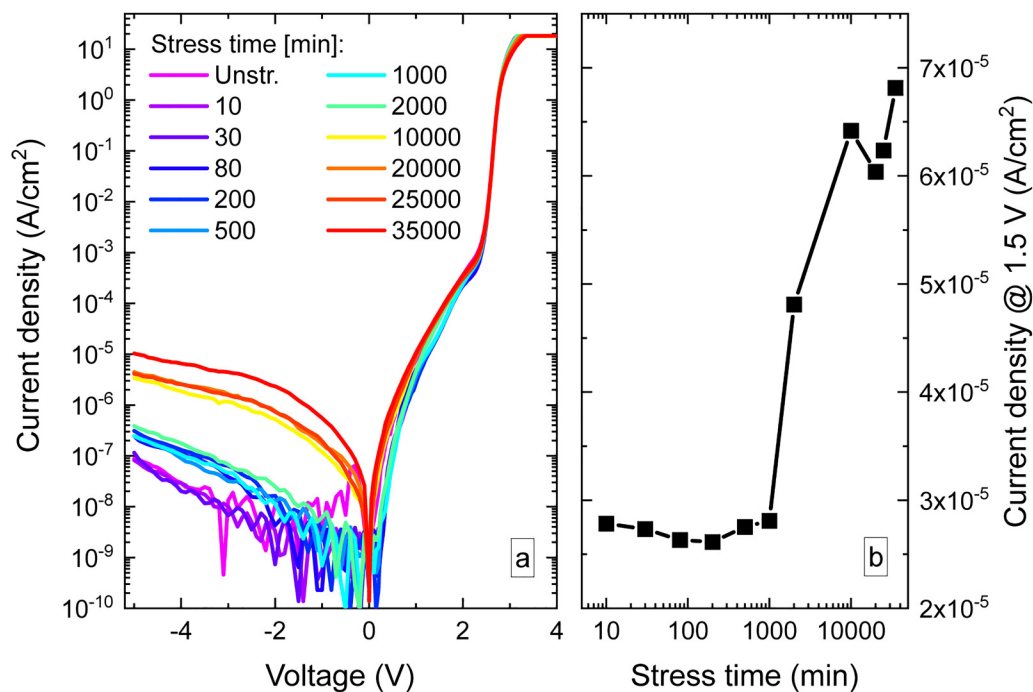


FIG. 2. I-V characterizations of the device after each step of the stress (a) and the current density at 1.5 V (b).

dominated by the Bn^2 term, and the efficiency becomes insensitive on the density of defects. This explains analytically why the optical power and efficiency curves in Fig. 3 show variations only at low current levels.

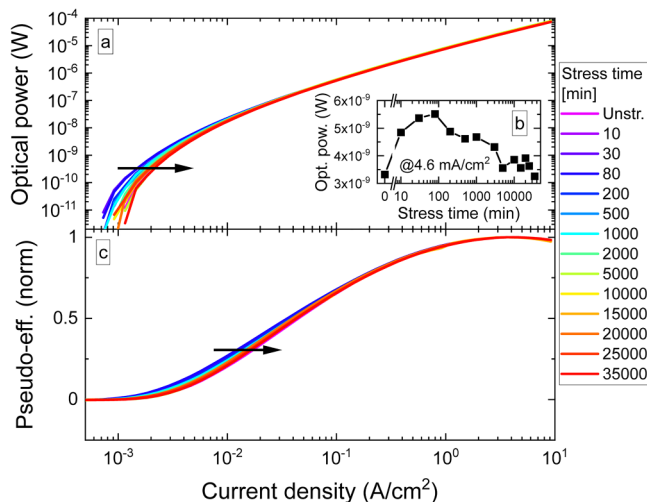


FIG. 3. Optical power-current (L-I) characterizations after each step of the stress (a), optical power at 4.6 mA/cm^2 with respect to the stress time (b), and pseudo-efficiency calculated from L-I characterizations and normalized by the maximum value (c).

At high current levels, the effect of non-radiative defects is not visible because the recombination rate is dominated by the bimolecular recombination components. This is demonstrated by the fact that optical power has a nearly linear ($OP \sim I^{1.16}$) dependence on current (the almost linear dependence of current confirms that Auger recombination is playing a minor role, in the analyzed current range, which is below the IQE peak).

To better understand the physical origin of degradation, we analyzed the charge distribution near the junction through capacitance-voltage profiling [Fig. 4(a)], which showed modification after stress. The charge density profile [Fig. 4(b)] was calculated from C-V measurements: it is possible to see a weakly doped region (up to 175 nm, region 1) with a charge density of $1 \times 10^{17} \text{ cm}^{-3}$, an intrinsic region (175–250 nm, charge density $5 \times 10^{16} \text{ cm}^{-3}$, region 2), and a highly doped zone (over 250 nm, charge density $2 \times 10^{17} \text{ cm}^{-3}$, region 3). During the stress, the density of free carriers in the region closer to the junction was found to show a gradual increase, possibly due to the creation of shallow trap states, resulting in an enhancement of free carriers. This is clearly visible by looking at the integral of charge distributions in the region 175–275 nm, plotted in Fig. 4(c).

To identify the generation of defects induced by stress experiments, steady-state photocapacitance measurements were performed on the device: the device under test was kept under dark for 200 s to fill all defects. After this initial phase, the device was illuminated with monochromatic light for 100 s to deplete the defects, and the corresponding capacitance transient was measured. The sample was then put again in dark, and exposed to positive bias,

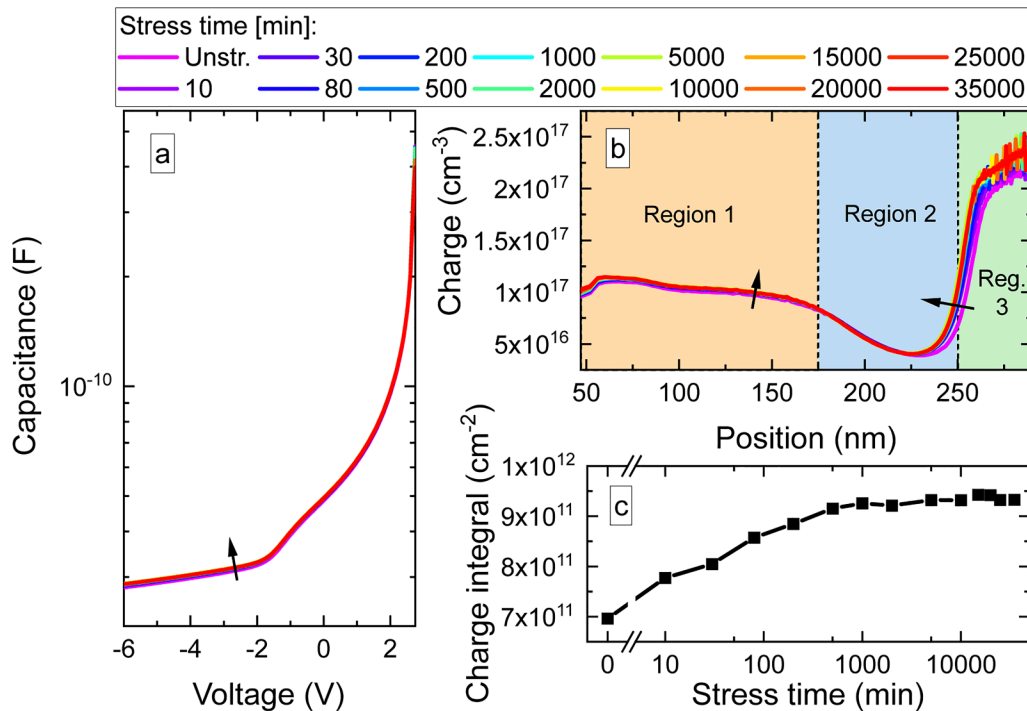


FIG. 4. C–V characterizations after each step of the stress (a), the charge profile with respect to the position calculated from C–V characterizations (b) and the charge integral in the region 175–275 nm (c).

to fill the defects again.¹⁷ From the analysis of the capacitance transients, we were able to extract SSPC curves in Fig. 5(a). As can be noticed, it is possible to identify two energy levels: T_1 has a transition energy around 1.3 eV and corresponds to a near-midgap state, while T_2 has a transition energy around 2.2 eV. The slope change visible around 2.75 eV is due to the absorption by the quantum wells. As can be noticed, stress induced a change in the signal associated with trap T_2 , whose signal was found to decrease in the initial 1000 min of stress, possibly due to an annealing phase, and then increase again [Fig. 5(b)]. The increase in the concentration of deep defects detected for times longer than 1000 min can be responsible for the increase in the leakage current detected in the same interval [see Fig. 2(b)], consistently with recent reports on the impact of deep defects on sub-turn-on leakage current.^{14,15}

To quantify the impact of stress on the performance of the quantum wells, the device was characterized by photoluminescence before and after the stress under 405 nm resonant excitation. The spatially resolved emission was measured in the range between 420 and 700 nm. In Fig. 6, the photoluminescence emission at 430 nm (the device nominal emission wavelength) is plotted. By comparing the emission before [Fig. 6(b)] and after [Fig. 6(c)] the stress, it is possible to see that there is a strong decrease in luminescence, which is stronger in the region stressed under the laser beam. From the plot of the ratio between the photoluminescence signal before and after the stress [Fig. 6(d)], it is possible to see that the signal is lowered by a factor of around 2 on the whole device

except for a very small region in which the signal is lowered by a factor of almost 4. By looking at the intensity profile of the laser beam in Fig. 6(e), it is evident that this region perfectly matches the area on which the laser beam was focused [see Fig. 6(f)], but there is a non-negligible amount of light coming also in the region outside the laser spot. Therefore, we can conclude that the optical stress induced a general decrease in the photoluminescence of the device, with a stronger effect in the area of highest excitation.

The photoluminescence signal was integrated over the device area and plotted in Fig. 7 at different excitation intensities. Here, it is possible to see a peak in luminescence emission at 430 nm, which is the nominal emission wavelength of the device. There is a decrease in luminescence in the stressed device; this decrease is lower at higher luminescence excitation densities. There is also an emission at wavelengths longer than 500 nm, which is a well-known yellow emission by gallium nitride that is ascribed to gallium vacancies¹⁸ or their complexes with carbon^{19–21} or nitrogen.^{22,23}

By looking at the ratio between the luminescence before and after the stress at different excitation intensities (Fig. 8), it is possible to note that the photoluminescence signal around the emission peak decreases after the stress (i.e., the post/pre ratio is lower than unit), as noted before. This decrease is inversely proportional to the photoluminescence excitation intensity. For longer wavelengths, in the yellow/red spectral range, it is possible to see that at low excitation intensities, there is a decrease in the signal after the stress, whereas at high excitation densities, there is an increase in the

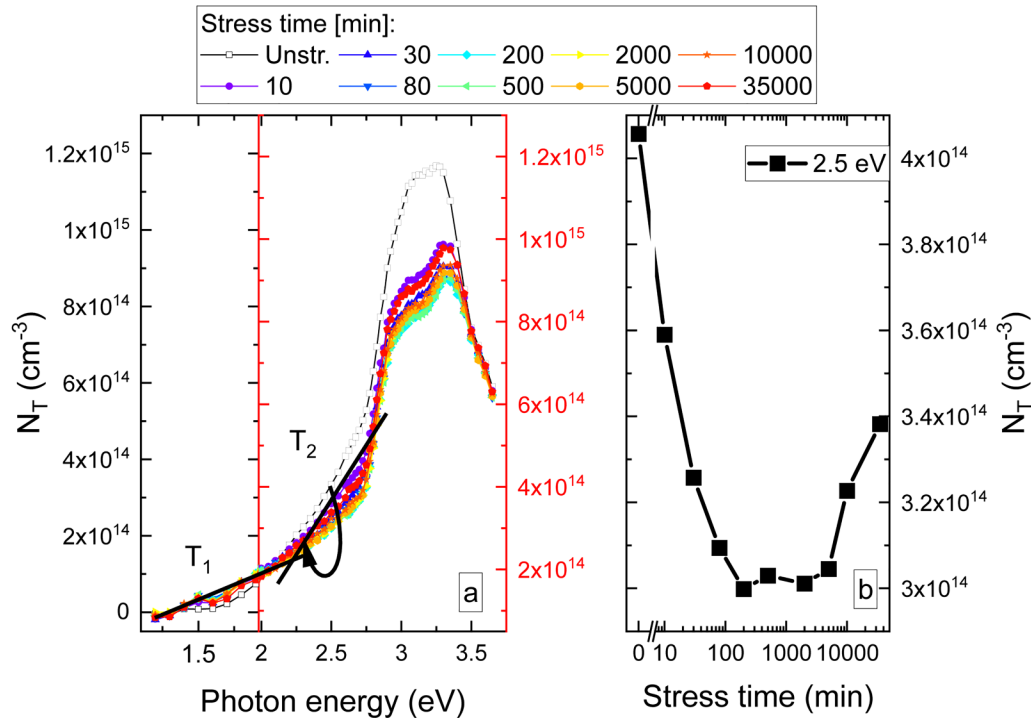


FIG. 5. Trap level density N_T calculated from SSPC and C-V measurements (a) and the trap level density at 2.5 eV (b).

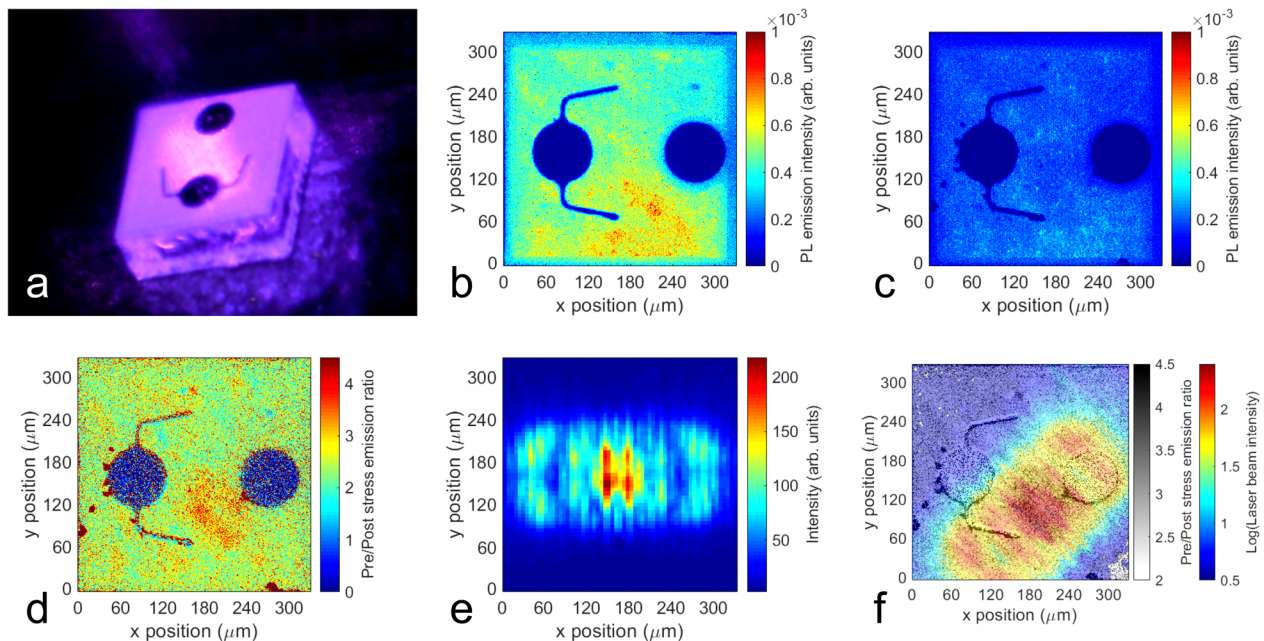


FIG. 6. (a) Optical image of the device with a laser beam. (b) Photoluminescence map of the unstressed device. (c) Photoluminescence map of the 35 000 min stressed device. (d) Pre/post-ratio of the photoluminescence maps. (e) Laser beam intensity profile. (f) Laser beam profile [colored region, logarithmic scale, corresponding to (e)] rotated and superimposed to the pre/post-photoluminescence map [grayscale, corresponding to (d)].

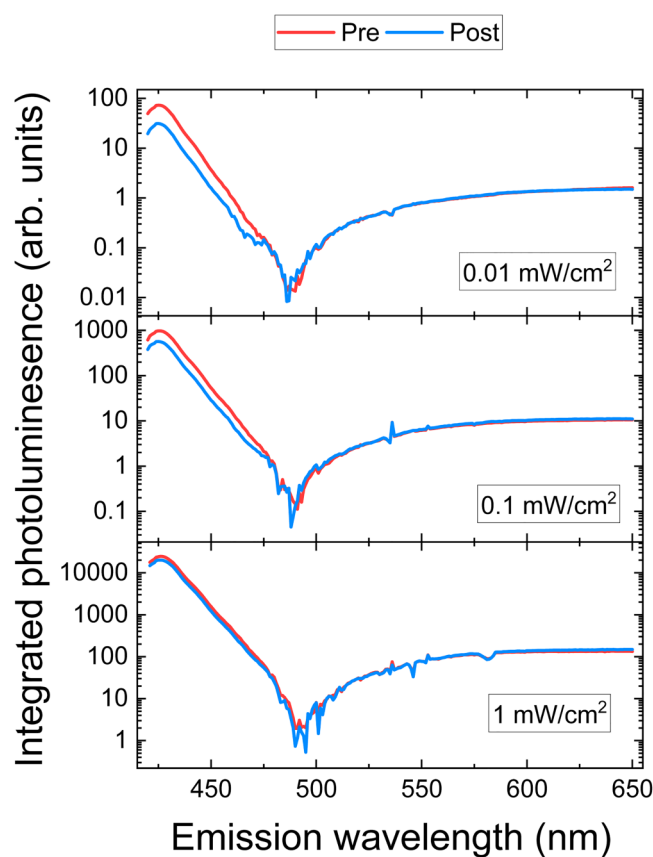


FIG. 7. Photoluminescence signal, integrated over the device area, with respect to emission wavelengths at 0.01, 0.1, and 1 mW/cm² excitation intensity at 405 nm.

luminescence signal (i.e., the post/pre ratio is higher than unity). This can be attributed to the creation of new defects in the devices: relatively shallow levels ($E_C - 2.2$ eV), corresponding to the T_2 state detected by SSPC measurements, are expected to cause an increase in yellow luminescence, whereas deeper trap levels (possibly near midgap, 1.3 eV) are known to increase non-radiative Shockley–Read–Hall recombination.²⁴ At low excitation densities, the increased SRH recombination causes a decrease in luminescence at all the wavelengths. At high excitation levels, trap states are saturated. There is only a small decrease in luminescence at 430 nm due to increased SRH recombination, whereas the increase in shallow trap levels causes an increase in yellow luminescence after the stress.

With regard to the origin of the degradation process, since the device is stressed in an open-circuit condition, it cannot be directly attributed to the flow of current. We suggest that the increase in the concentration of deep states is favored by the energy released by non-radiative recombination events: at high laser beams (i.e., at an optical power of 0.766 W at 405 nm, which corresponds to a carrier generation rate around 10^{27} cm⁻³/s, assuming that the optical radiation is fully absorbed by an active region of 10 nm thickness and

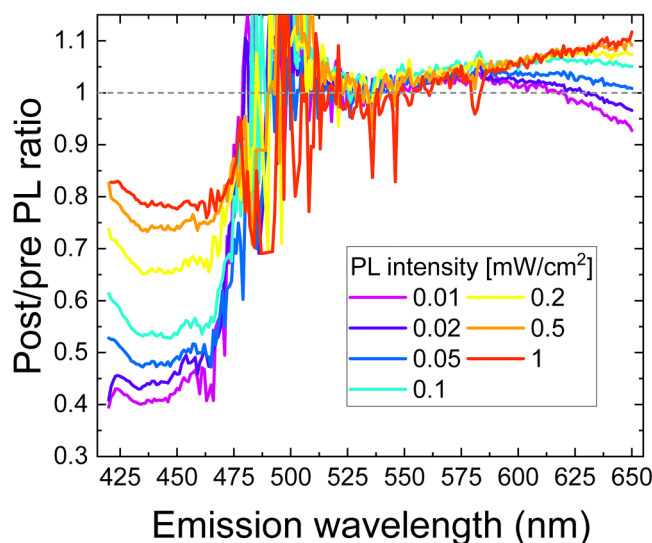


FIG. 8. Integrated photoluminescence ratio between a 35 000 min stressed device and an unstressed device with respect to emission wavelengths at different excitation intensities.

$330 \times 330 \mu\text{m}^2$ area), Auger recombination is supposed to prevail on SRH recombination. The SRH recombination rate is proportional to An , with the recombination rate around 2×10^{25} cm⁻³/s, whereas the Auger recombination rate is proportional to Cn^3 , obtaining a recombination rate around 6×10^{26} cm⁻³/s, assuming $A = 10^6$ 1/s, $B = 10^{-12}$ cm³/s, and $C = 10^{-31}$ cm⁶/s.²⁵ We, therefore, suggest that Auger recombination plays the strongest role. Each Auger recombination event releases an energy around 2.7 eV, which is larger than the expected threshold for the generation of midgap states, which are typically ascribed to gallium vacancy complexes with hydrogen,²⁶ nitrogen vacancies,¹² and $V_{\text{Ga}}-V_{\text{N}}$ complexes.²⁷

CONCLUSIONS

In this work, we demonstrated that GaN-based LEDs can show optically induced degradation and characterized the related phenomena. Devices were stressed with a high power 405 nm laser in an open-circuit condition, and we observed a strong decrease in photoluminescence in the area illuminated by the laser beam. To understand the physical origin of this degradation, we performed a detailed characterization, and we observed an increase in low forward bias current, which can be ascribed to increased tunneling mechanisms and a decrease in quantum efficiency, especially at low currents. C–V measurements showed an increase in charge during the stress, while SSPC measurements showed two deep levels, one with a transition energy of 1.3 eV, thus near midgap (which is supposed to be related to optical degradation), and another one with a transition energy of around 2.2 eV, possibly related to gallium vacancies and its complexes with nitrogen and carbon. In conclusion, we attributed the degradation to the presence of a near-midgap deep level, which causes non-radiative SRH recombination and thus lowers luminescence and quantum efficiency.

ACKNOWLEDGMENTS

This research was partly performed within the project Internet of Things: Sviluppi Metodologici, Tecnologici e Applicativi, co-founded (2018–2022) by the Italian Ministry of Education, Universities and Research (MIUR) under the aegis of the “Fondo per il finanziamento dei dipartimenti universitari di eccellenza” initiative (Law 232/2016).

AUTHOR DECLARATIONS

Conflict of Interest

The authors have no conflicts to disclose.

DATA AVAILABILITY

The data that support the findings of this study are available from the corresponding author upon reasonable request.

REFERENCES

- ¹M.-H. Chang, D. Das, P. V. Varde, and M. Pecht, “Light emitting diodes reliability review,” *Microelectron. Reliab.* **52**, 762–782 (2012).
- ²L. X. Zhao, E. J. Thrush, C. J. Humphreys, and W. A. Phillips, “Degradation of GaN-based quantum well light-emitting diodes,” *J. Appl. Phys.* **103**, 024501 (2008).
- ³L. Liu, M. Ling, J. Yang, W. Xiong, W. Jia, and G. Wang, “Efficiency degradation behaviors of current/thermal co-stressed GaN-based blue light emitting diodes with vertical-structure,” *J. Appl. Phys.* **111**, 093110 (2012).
- ⁴M. Meneghini, L.-R. Trevisanello, U. Zehnder, G. Meneghesso, and E. Zanoni, “Reversible degradation of ohmic contacts on p-GaN for application in high-brightness LEDs,” *IEEE Trans. Electron Devices* **54**, 3245–3251 (2007).
- ⁵D. Cherns, S. J. Henley, and F. A. Ponce, “Edge and screw dislocations as non-radiative centers in InGaN/GaN quantum well luminescence,” *Appl. Phys. Lett.* **78**, 2691–2693 (2001).
- ⁶Q. Dai, M. F. Schubert, M. H. Kim, J. K. Kim, E. F. Schubert, D. D. Koleske, M. H. Crawford, S. R. Lee, A. J. Fischer, G. Thaler, and M. A. Banas, “Internal quantum efficiency and nonradiative recombination coefficient of GaInN/GaN multiple quantum wells with different dislocation densities,” *Appl. Phys. Lett.* **94**, 111109 (2009).
- ⁷N. Renso, M. Meneghini, M. Buffolo, C. De Santi, G. Meneghesso, and E. Zanoni, “Understanding the degradation processes of GaN based LEDs submitted to extremely high current density,” *Microelectron. Reliab.* **76–77**, 556–560 (2017).
- ⁸P. Tian, A. Althumali, E. Gu, I. M. Watson, M. D. Dawson, and R. Liu, “Aging characteristics of blue InGaN micro-light emitting diodes at an extremely high current density of 3.5 kA cm^{-2} ,” *Semicond. Sci. Technol.* **31**, 045005 (2016).
- ⁹M. Meneghini, S. Podda, A. Morelli, R. Pintus, L. Trevisanello, G. Meneghesso, M. Vanzi, and E. Zanoni, “High brightness GaN LEDs degradation during dc and pulsed stress,” *Microelectron. Reliab.* **46**, 1720–1724 (2006).
- ¹⁰M. Dal Lago, M. Meneghini, N. Trivellin, G. Mura, M. Vanzi, G. Meneghesso, and E. Zanoni, “Phosphors for LED-based light sources: Thermal properties and reliability issues,” *Microelectron. Reliab.* **52**, 2164–2167 (2012).
- ¹¹M. Meneghini, M. Dal Lago, N. Trivellin, G. Mura, M. Vanzi, G. Meneghesso, and E. Zanoni, “Chip and package-related degradation of high power white LEDs,” *Microelectron. Reliab.* **52**, 804–812 (2012).
- ¹²C. G. Van de Walle, “Interactions of hydrogen with native defects in GaN,” *Phys. Rev. B* **56**, R10020–R10023 (1997).
- ¹³OSRAM OSTAR[®] LE B P3MQ datasheet.
- ¹⁴M. Auf der Maur, B. Galler, I. Pietzonka, M. Strassburg, H. Lugauer, and A. Di Carlo, “Trap-assisted tunneling in InGaN/GaN single-quantum-well light-emitting diodes,” *Appl. Phys. Lett.* **105**, 133504 (2014).
- ¹⁵M. Mandurro, G. Verzellesi, M. Goano, M. Vallone, F. Bertazzi, G. Ghione, M. Meneghini, G. Meneghesso, and E. Zanoni, “Physics-based modeling and experimental implications of trap-assisted tunneling in InGaN/GaN light-emitting diodes,” *Phys. Status Solidi A* **212**, 947–953 (2015).
- ¹⁶N. Roccatto, F. Piva, C. De Santi, R. Brescancin, K. Mukherjee, M. Buffolo, C. Haller, J.-F. Carlin, N. Grandjean, M. Vallone, A. Tibaldi, F. Bertazzi, M. Goano, G. Verzellesi, G. Meneghesso, E. Zanoni, and M. Meneghini, “Modeling the electrical characteristics of InGaN/GaN LED structures based on experimentally-measured defect characteristics,” *J. Phys. D: Appl. Phys.* **54**, 425105 (2021).
- ¹⁷A. Armstrong, T. A. Henry, D. D. Koleske, M. H. Crawford, K. R. Westlake, and S. R. Lee, “Dependence of radiative efficiency and deep level defect incorporation on threading dislocation density for InGaN/GaN light emitting diodes,” *Appl. Phys. Lett.* **101**, 162102 (2012).
- ¹⁸P. Kamyczek, E. Placzek-Popko, V. Kolkovsky, S. Grzanka, and R. Czernecki, “A deep acceptor defect responsible for the yellow luminescence in GaN and AlGaIn,” *J. Appl. Phys.* **111**, 113105 (2012).
- ¹⁹J. L. Lyons, A. Janotti, and C. G. Van de Walle, “Effects of carbon on the electrical and optical properties of InN, GaN, and AlN,” *Phys. Rev. B* **89**, 035204 (2014).
- ²⁰J. L. Lyons, A. Janotti, and C. G. Van De Walle, “Carbon impurities and the yellow luminescence in GaN,” *Appl. Phys. Lett.* **97**, 152108 (2010).
- ²¹T. Ogino and M. Aoki, “Mechanism of yellow luminescence in GaN,” *Jpn. J. Appl. Phys.* **19**, 2395–2405 (1980).
- ²²J. Neugebauer and C. G. Van de Walle, “Gallium vacancies and the yellow luminescence in GaN,” *Appl. Phys. Lett.* **69**, 503–505 (1996).
- ²³A. Sedhain, J. Li, J. Y. Lin, and H. X. Jiang, “Nature of deep center emissions in GaN,” *Appl. Phys. Lett.* **96**, 151902 (2010).
- ²⁴W. Shockley and W. T. Read, “Statistics of the recombinations of holes and electrons,” *Phys. Rev.* **87**, 835–842 (1952).
- ²⁵A. David, N. G. Young, C. A. Hurni, and M. D. Craven, “Quantum efficiency of III-nitride emitters: Evidence for defect-assisted nonradiative recombination and its effect on the green gap,” *Phys. Rev. Appl.* **11**, 031001 (2019).
- ²⁶C. E. Dreyer, A. Alkauskas, J. L. Lyons, J. S. Speck, and C. G. Van De Walle, “Gallium vacancy complexes as a cause of Shockley-Read-Hall recombination in III-nitride light emitters,” *Appl. Phys. Lett.* **108**, 141101 (2016).
- ²⁷S. F. Chichibu, A. Uedono, K. Kojima, H. Ikeda, K. Fujito, S. Takashima, M. Edo, K. Ueno, and S. Ishibashi, “The origins and properties of intrinsic non-radiative recombination centers in wide bandgap GaN and AlGaIn,” *J. Appl. Phys.* **123**, 161413 (2018).